NUKLEONIKA 2015;60(1):109–114
doi: 10.1515/nuka-2015-0022

ORIGINAL PAPER

DE GRUYTER
OPEN

Structure and Mössbauer spectroscopy studies of mechanically activated $(BiFeO_3)_{1-x}$-$(BaTiO_3)_x$ solid solutions

**Bożena Malesa,
Anna Antolak-Dudka,
Dariusz Oleszak,
Tomasz Pikula**

Abstract. $(BiFeO_3)_{1-x}$-$(BaTiO_3)_x$ solid solutions with x = 0.1–0.4 and 0.7 were investigated. The ceramics were prepared by mechanical activation technology and subsequent heat treatment. As was proved by X-ray diffraction, increase of $BaTiO_3$ concentration causes a change in the crystalline structure from the rhombohedral structure characteristic of $BiFeO_3$ to a cubic one. ^{57}Fe Mössbauer spectroscopy allowed observation of a gradual transformation from an ordered spin structure of Fe^{3+} ions to the paramagnetic state with an increase of x.

Key words: ceramic solid solutions • hyperfine interactions • mechanical activation • Mössbauer spectroscopy

B. Malesa
Institute of Electronics and Information Technology,
Lublin University of Technology,
38A Nadbystrzycka Str., 20-618 Lublin, Poland
and Department and Division of Nuclear Medicine,
Lublin University of Medicine,
8 Jaczewskiego Str., 20-954 Lublin, Poland

A. Antolak-Dudka, D. Oleszak
Faculty of Materials Science and Engineering,
Warsaw University of Technology,
141 Wołoska Str., 02-507 Warsaw, Poland

T. Pikula✉
Institute of Electronics and Information Technology,
Lublin University of Technology,
38A Nadbystrzycka Str., 20-618 Lublin, Poland,
Tel.: +48 81 538 4503, Fax: +48 81 538 4312,
E-mail: t.pikula@pollub.pl

Received: 18 June 2014
Accepted: 2 November 2014

Introduction

Materials simultaneously exhibiting ferroelectric and ferro-/antiferromagnetic and/or ferroelastic properties, that is multiferroics, are the subject of intensive research due to their potential applications in new types of magnetoelectric devices, next-generation memory storage materials, or sensors of magnetic field [1, 2]. Until now, the best recognized single-phase multiferroic compound is bismuth ferrite, $BiFeO_3$, in which the ferroelectric and antiferromagnetic ordering coexist at ambient temperature. However, during synthesis of $BiFeO_3$, the formation of undesired secondary phases occurs, and the crystalline structure is often not stable. To improve structural properties, solid solutions of bismuth ferrite with stable ferroelectrics, for example, barium titanate, are synthesized.

$BiFeO_3$ crystallizes with a rhombohedrally distorted perovskite-like structure described by the *R*3*c* space group. At room temperature, it is a G-type antiferromagnet with a canted spin structure. Moreover, it appears as a spin cycloid with a period of approximately 62 nm, which cancels the net macroscopic magnetization expected in a canted antiferromagnet [3]. Most current investigation tend to destroy the spin cycloid and release the inherent magnetization in order to improve multiferroic properties of $BiFeO_3$ [4]. This may be achieved, for example, by structural modifications or deformations introduced by cation substitution or doping [5]. Therefore, a solid solution of $BiFeO_3$ with $BaTiO_3$ results in improved ferroelectric properties as well as enhanced magnetic properties. As recently

reported, $(BiFeO_3)_{1-x}$-$(BaTiO_3)_x$ solid solutions exhibit magnetoelectric coupling within a narrow composition range, that is, x = 0.20–0.29, what provides a possibility of developing electrically or magnetically tunable thin-film devices [6].

The standard method for preparation of $(BiFeO_3)_{1-x}$-$(BaTiO_3)_x$ solid solutions is the solid-state sintering. Another promising technology is the mechanical activation (MA), where the prolonged milling process provides the material in the nanocrystalline or amorphous state. The subsequent thermal treatment completes the solid-state reaction and allows us to obtain the desired solid solutions. The MA process has several advantages over the standard solid-state sintering method. First, it skips the calcination step at an intermediate temperature, which simplifies the process. Second, the mechanically derived powders possess higher sinterability than powders synthesized by a conventional solid-state reaction. Preparing materials with the MA method seems to be promising at an industrial scale due to its simplicity and relatively low cost of processing.

In the present work, the samples of $(BiFeO_3)_{1-x}$-$(BaTiO_3)_x$ solid solutions with x = 0.1–0.4 and 0.7 prepared by the MA and subsequent heat treatment were investigated. This is a continuation of our previous studies published elsewhere [7]. Compared to the previous work, current investigation covers a wider range of $BaTiO_3$ concentrations. Therefore, it becomes possible to clearly observe structural as well as magnetic transformation with the increase of $BaTiO_3$ content and to draw more general conclusions regarding the hyperfine interactions of ^{57}Fe nuclei located in $(BiFeO_3)_{1-x}$-$(BaTiO_3)_x$. The aim of the present study was: (1) to show that MA combined with additional thermal treatment may be used as a technology for production of $(BiFeO_3)_{1-x}$-$(BaTiO_3)_x$ solid solutions with relatively low concentration of impurities and (2) to study the influence of $BaTiO_3$ content on the type of crystalline lattice and the type of magnetic ordering as well as on hyperfine interaction parameters of the investigated solid solutions.

Experimental details

Analytical reagent grade 99.9% pure oxides of α-Bi_2O_3 and α-Fe_2O_3 and barium titanate $BaTiO_3$ were used as precursor materials in order to obtain $(BiFeO_3)_{1-x}$-$(BaTiO_3)_x$ solid solutions with x = 0.1–0.4 and 0.7, according to the following reaction:

$$(Bi_2O_3)_{(1-x)/2} + (Fe_2O_3)_{(1-x)/2} + (BaTiO_3)_x \rightarrow (BiFeO_3)_{1-x}\text{-}(BaTiO_3)_x$$

The powder mixture was weighted and milled in a high-energy ball mill type Fritsch Pulverisette P5 with stainless steel balls of 10 mm diameter. The ball-to-powder weight ratio was 10:1. Milling processes were performed under air atmosphere for 2, 5, 10, 20, 50 and 100 h. After MA subsequent thermal treatment was carried out in order to complete the solid-state reaction. As reported in our earlier works, the gradual heating from room temperature to 993 K [8] as well as isothermal annealing at 1073 K [7] were not the appropriate thermal processes to obtain the desired $(BiFeO_3)_{1-x}$-$(BaTiO_3)_x$ solid solutions. Therefore, in the present work, the isothermal annealing at 1173 K for 1 h in air was applied to complete the solid-state reaction.

X-ray diffraction (XRD) measurements were carried out at room temperature using a RIGAKU Miniflex2 diffractometer working in a continuous scanning mode with CuK_α radiation. Measurements of the ^{57}Fe Mössbauer spectra were made using transmission geometry with a 10-mCi source of ^{57}Co in a rhodium matrix. The spectrometer was calibrated using α-Fe foil at room temperature.

Results and discussion

The process of formation of $(BiFeO_3)_{1-x}$-$(BaTiO_3)_x$ solid solutions was monitored by XRD (X-ray diffraction) and Mössbauer spectroscopy (MS) techniques. XRD studies conducted at every stage of the MA process (from 2 to 100 h) showed that the peaks attributed to constituents α-Bi_2O_3, α-Fe_2O_3, and $BaTiO_3$ are shifted, overlapped, broadened, reduced in their intensity, or disappear with an increase of milling time as shown in Fig. 1 for the selected compositions. In all XRD patterns of the $0.6BiFeO_3$-$0.4BaTiO_3$ solid solution (Fig. 1a), the broadened halo is visible within the range of 2Θ = 24°–35°, which may be associated with a progressive fragmentation and/or partial amorphization of the precursors. The diffraction peaks visible in the diffractogram for the sample milled for 100 h originate probably from the $Bi_2Fe_4O_9$ phase (the main peak at 2Θ = 27.2°) and unreacted α-Bi_2O_3, $BaTiO_3$, and α-Fe_2O_3. It may be concluded that during the MA process the desired $0.6BiFeO_3$-$0.4BaTiO_3$ solid solution was not formed. In the case of a $0.3BiFeO_3$-$0.7BaTiO_3$ solid solution (Fig. 1b), a weak halo within the range of 2Θ = 27°–32° is still visible; moreover, the arrangement of diffraction peaks is different from that in the previous sample. Now the peak with highest intensity is visible for 2Θ = 31.5°, and the majority of peaks have the same angular positions as the cubic type of $BaTiO_3$. It means that probably the $0.3BiFeO_3$-$0.7BaTiO_3$ solid solution with a cubic lattice starts to form during the MA process; however, a small amount of unreacted α-Bi_2O_3 and α-Fe_2O_3 still exists within the sample.

Heat treatment changes the situation clearly. Isothermal annealing at 1173 K allowed us to obtain $(BiFeO_3)_{1-x}$-$(BaTiO_3)_x$ solid solutions with relatively low amount of impurities. With increasing content of $BaTiO_3$, structural crystallographic changes occur in the resultant $(BiFeO_3)_{1-x}$-$(BaTiO_3)_x$ solid solutions. As reported in Refs. [5, 6, and references therein], rhombohedral symmetry is maintained for x = 0–0.3, after which cubic symmetry predominates up to x = 0.93. For x > 0.93 and for a pure $BaTiO_3$ compound, the structure is tetragonal.

In the case of our studies, the structural transformation from rhombohedral (*R*3*c* space group) to cubic symmetry (*Pm*3*m* space group) probably

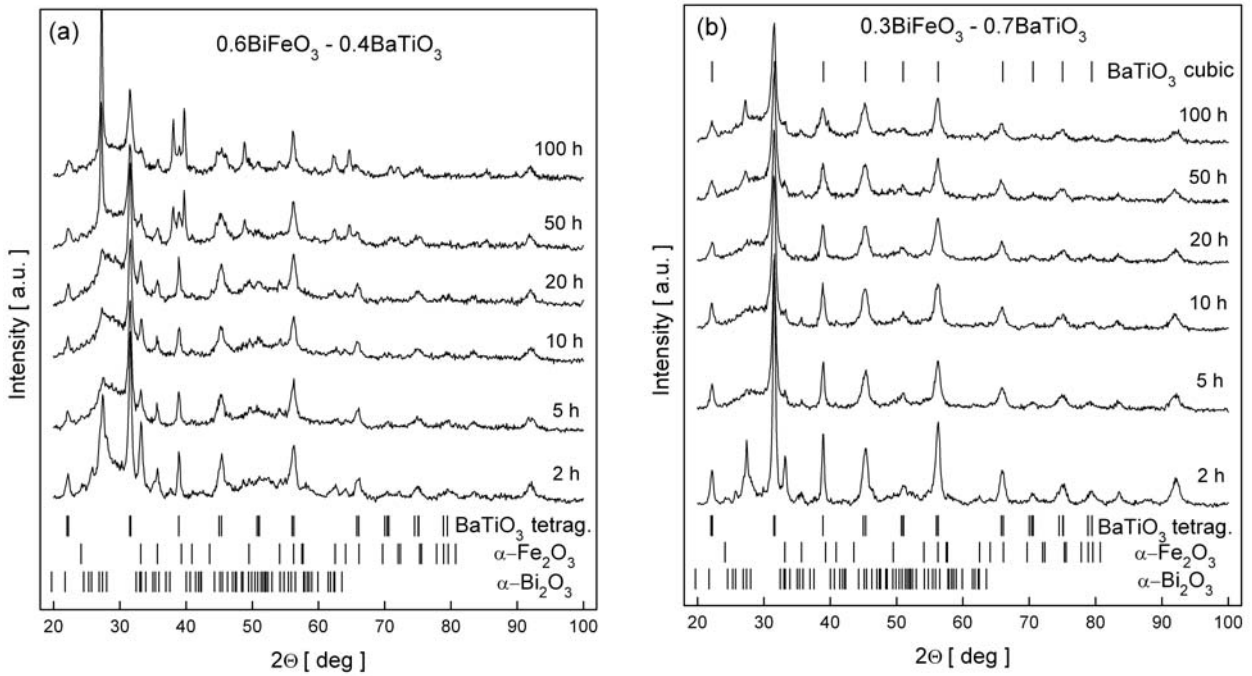

Fig. 1. X-ray diffraction patterns for (a) $0.6BiFeO_3$-$0.4BaTiO_3$ and (b) $0.3BiFeO_3$-$0.7BaTiO_3$ solid solutions after mechanical activation for various periods; positions of diffraction lines for α-Bi_2O_3, α-Fe_2O_3, and $BaTiO_3$ (tetragonal and cubic type) are marked according to PDF card no. 00-027-0053, 01-073-2234, 01-075-0462, and 01-075-0461, respectively.

occurs for $x \geq 0.4$. Similar, gradual transformation was observed for $(BiFeO_3)_{1-x}$-$(SrTiO_3)_x$ solid solutions in Ref. [9], where the structural transformation proceeded for $x = 0.5$–0.7 with the multiphase region in between. As shown in Fig. 2, the angular positions of diffraction lines are similar for all the compositions. Besides XRD patterns for the samples, the positions of diffraction lines for rhombohedral phase (i.e., pure $BiFeO_3$) as well as for cubic phase (i.e., cubic-type $BaTiO_3$) are marked. The evidence for the structural change from rhombohedral to cubic is the disappearance of the splitting of diffraction peaks with increase of x. This effect may be observed when we focus on the peaks (110), (111), (210), (211), and (220) presented in Fig. 3a–e for all the compositions. It is visible that the splitting of diffraction lines gradually disappears as the content of $BaTiO_3$ increases from $x = 0.1$ to 0.4. The peaks are clearly shifted toward lower 2Θ angles. This effect is due to the substitution of Bi^{3+} (ionic radius: 1.08 Å) and Fe^{3+} (0.64 Å) ions by larger Ba^{2+} (1.35 Å) and Ti^{4+} (0.68 Å) ions resulting in the lattice expansion. The values of the lattice parameters were determined after $K\alpha_2$ stripping using the Rachinger method [10] and applying the DHN PDS numerical program.

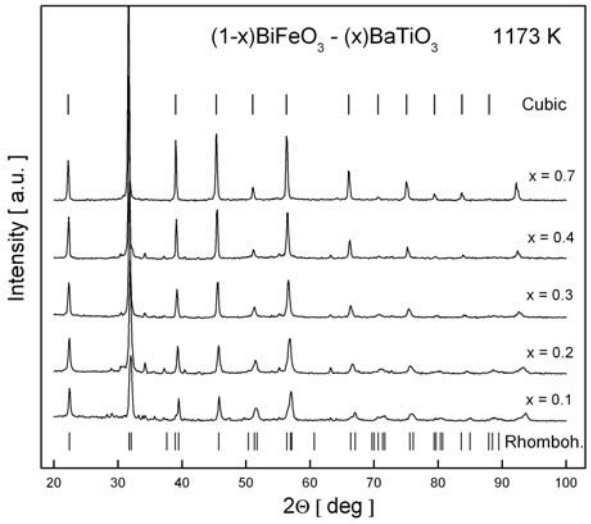

Fig. 2. X-ray diffraction patterns for $(BiFeO_3)_{1-x}$-$(BaTiO_3)_x$ solid solutions after 100 h MA and isothermal annealing at 1173 K; positions of diffraction lines for rhombohedral and cubic phases are marked according to PDF card no. 01-082-1254 and 01-075-0461, respectively.

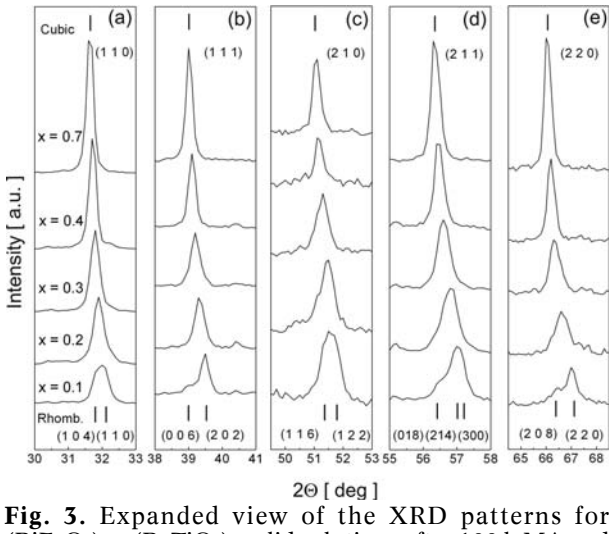

Fig. 3. Expanded view of the XRD patterns for $(BiFeO_3)_{1-x}$-$(BaTiO_3)_x$ solid solutions after 100 h MA and isothermal annealing at 1173 K; positions of diffraction lines for rhombohedral and cubic phases are marked according to PDF card no. 01-082-1254 and 01-075-0461, respectively.

Table 1. Structural parameters of $(BiFeO_3)_{1-x}$-$(BaTiO_3)_x$ solid solutions prepared by mechanical activation and isothermal annealing at 1173 K: a, b, c, α, β, γ – lattice parameters; V – volume of elemental cell; uncertainty of the values are given in parentheses for the last significant number

x	Space group	$a = b$ [Å]	c [Å]	α [°]	β [°]	γ [°]	V [Å^3]
0 $BiFeO_3$	*R3c*	5.581	13.876	90	90	120	432.20
0.1	*R3c*	5.5887(20)	13.7756(40)	90	90	120	430.26
0.2	*R3c*	5.6105(35)	13.7756(70)	90	90	120	433.62
0.3	*R3c*	5.6370(20)	13.7996(40)	90	90	120	438.49
		$a = b = c$ [Å]					
0.4	*Pm3m*	3.9924(31)		90	90	90	63.71
0.7	*Pm3m*	3.9993(28)		90	90	90	64.09

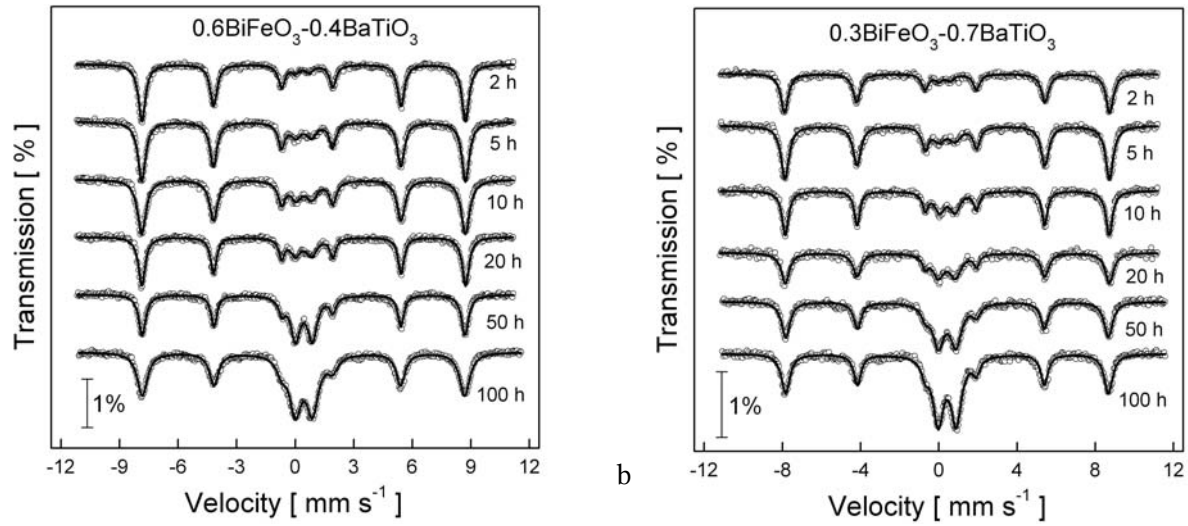

Fig. 4. Fitted room-temperature Mössbauer spectra of (a) $0.6BiFeO_3$-$0.4BaTiO_3$ and (b) $0.3BiFeO_3$-$0.7BaTiO_3$ as a function of milling time.

The obtained results are listed in Table 1 and agree well with the data reported for $(BiFeO_3)_{1-x}$-$(BaTiO_3)_x$ solid solutions prepared using other methods, that is, molten salt and solid-state sintering, respectively [5, 11]. It may be stated that increasing concentration of $BaTiO_3$ did not change the crystallographic system up to $x = 0.3$; however, a noticeable increase in volume of elemental cell occurred.

Mössbauer spectroscopy studies confirmed the XRD results. Room-temperature MS spectra are presented in Fig. 4 for the selected compositions of solid solutions as a function of milling time. For all the investigated compositions, similar MS spectra were registered, that is, they are all a superposition of a six-line pattern and a doublet in the central part of the spectrum. The numerical fitting was performed using one sextet and one doublet with the parameter χ^2 in the range of 1.1–2.0 (for $x = 0.1$), 1.0–1.8 ($x = 0.2$), 1.2–2.4 ($x = 0.3$), 1.1–1.9 ($x = 0.4$), and 1.0–1.6 ($x = 0.7$). Hyperfine interaction parameters determined from the fitting for the sextet are similar to the parameters for hematite (isomer shift relative to α-iron $\delta = 0.37(1)$ mm·s^{-1}, quadrupole shift $2\varepsilon = -0.20(2)$ mm·s^{-1}, and hyperfine magnetic field (HMF) induction $B_{hf} = 51.4$–51.8 T). This confirms the XRD results that the whole α-Fe_2O_3 did not react during the MA process with other precursors. The significant contribution of the sextet in each MS spectrum is associated with the large value of the Debye–Waller factor for hematite in comparison with other phases. For all the studied samples, the relative content of the hematite phase systematically decreases with the increase of milling time, and after 100 h, the contributions of both sextet and doublet are practically the same, about 50%. The second component of the MS spectra, that is, doublet, may be attributed to the paramagnetic compound $Bi_2Fe_4O_9$ (dibismuth tetrairon oxide). The values of the isomer shift and quadrupole splitting determined from the fitted spectra for the compositions $x = 0.1$–0.4 after 100 h of the MA process are practically the same, and they are as follows: $\delta \sim 0.31$ mm·s^{-1} and $\Delta = 0.84$–0.90 mm·s^{-1}. The obtained values are similar to those reported for $Bi_2Fe_4O_9$ in Ref. [12]. For $x = 0.7$, hyperfine interaction parameters for the paramagnetic component are slightly different, that is, $\delta = 0.28(1)$ mm·s^{-1} and $\Delta = 0.92(1)$ mm· s^{-1}. In this case, the doublet may come from the $0.3BiFeO_3$-$0.7BaTiO_3$ solid solution, which starts forming during the MA process. It may be added that the widths of the spectral lines for all the samples milled for 100 h are significantly larger than the natural one, which may be due to the small grain sizes, lattice deformation, and high level of internal strains in the mechanically treated material.

Room-temperature MS spectra for all the studied solid solutions obtained after isothermal annealing at 1173 K are presented in Fig. 5. It may be seen that

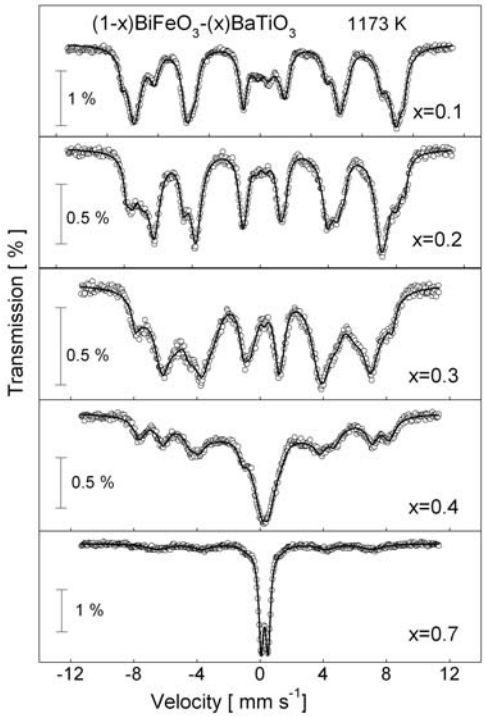

Fig. 5. Fitted room-temperature Mössbauer spectra of $(BiFeO_3)_{1-x}$-$(BaTiO_3)_x$ solid solutions after 100 h MA and isothermal annealing at 1173 K.

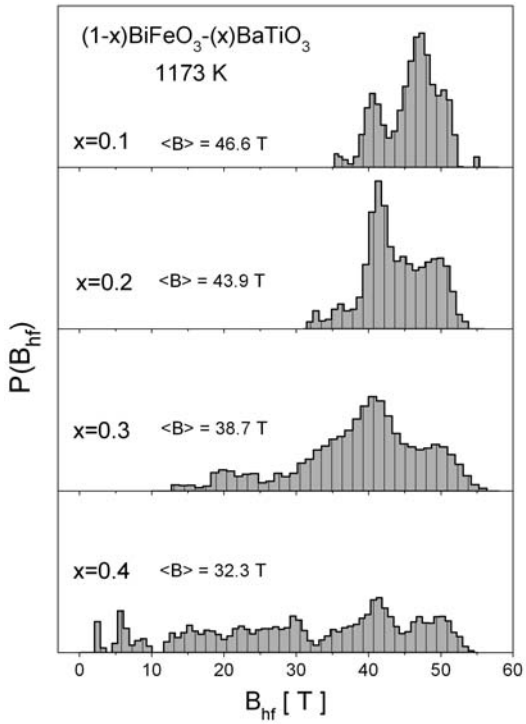

Fig. 6. Probability distribution of hyperfine magnetic field at ^{57}Fe nuclei located in $(BiFeO_3)_{1-x}$-$(BaTiO_3)_x$ solid solutions; $P(B_{hf})$: probability in arbitrary units.

the shape of the spectra is now more complicated. In the case of $x = 0.1$–0.4, the number of components of the spectra significantly increased. The change of magnetic ordering is clearly visible. The overall splitting of the outer absorption lines, which measures the average effective HMF at the ^{57}Fe nucleus, decreases by reflecting the weakening of the inherent strength of the magnetic interactions. For $x = 0.7$, the main phase is paramagnetic; however, a small magnetic background is still visible in the spectrum.

Numerical fitting was performed using both discrete and HMF distribution methods. In the fitting procedure using HMF distribution, the parameters for the doublet were fixed. From Fig. 6, it may be seen that the distributions are relatively broad and some maxima are more separated. The peak of hematite (field ~ 51 T) is visible in all distributions; however, its intensity is significantly smaller than that for other components and gradually disappears. The probability distributions of HMF appear most likely due to the random distribution of the diamagnetic Ti^{4+} ions around the ^{57}Fe nuclei. In Ref. [5], the authors proved that low concentration of $BaTiO_3$ dopants in $(BiFeO_3)_{1-x}$-$(BaTiO_3)_x$ solid solutions caused destruction of the spin cycloid and appearance of spontaneous magnetization. A further increase of $BaTiO_3$ concentration leads to decrease of saturation magnetization and finally transformation to the paramagnetic state. Furthermore, in the case of our samples, one can suppose that the increase of $BaTiO_3$ amount (decrease of Fe content) causes weakening of Fe-O-Fe superexchange interactions and increasing disorder in canted, antiferromagnetic spin alignment. This manifests by broadening of HMF distributions and decrease of $<B_{hf}>$ (values are given in Fig. 6). Based on XRD and MS studies it may be stated that the structural transformation to cubic symmetry is accompanied by a transition to the paramagnetic state. Our observation agrees well with the data reported in Ref. [9] for $(BiFeO_3)_{1-x}$-$(SrTiO_3)_x$ solid solutions, in which the structural transformation occurs in a similar concentration range. The parameters for the doublet observed for $x = 0.7$ have the values: $\delta = 0.39(1)$ mm·s^{-1} and $\Delta = 0.43(1)$ mm·s^{-1}. They are similar to those determined for a paramagnetic $0.5BiFeO_3$-$0.5BaTiO_3$ solid solution [5].

Conclusions

It was shown that it is possible to produce $(BiFeO_3)_{1-x}$-$(BaTiO_3)_x$ solid solutions employing MA technology with thermal treatment. X-ray diffraction and Mössbauer spectroscopy allowed us to monitor the technological process and obtain information about structure and magnetic properties of the studied materials. Mössbauer spectroscopy studies indicate that the increasing content of $BaTiO_3$ results in increasing disorder of spins in initial antiferromagnetic, canted alignment. Structural transformation from rhombohedral to cubic symmetry for $x = 0.4$–0.7 was proved by the disappearance of the splitting of diffraction peaks with increase of x. Moreover, the structural transformation to the cubic system is accompanied by the transition to the paramagnetic state.

Acknowledgments. Tomasz Pikula is a participant of the project: "Qualifications for the labour market-employer friendly university", co-financed by the European Union from European Social Fund.

References

1. Yin, Y. -W., Raju, M., Hu, W. -J., Weng, X. -J., Zou, K., Zhu, J., Li, X. -G., Zhang, Z. -D., & Li, Q. (2012). Multiferroic tunnel junctions. *Front. Phys.*, *7*, 380–385. DOI: 10.1007/s11467-012-0266-8.
2. Surowiak, Z., & Bochenek, D. (2007). Ferroikowe materiały inteligentne. *Elektronika*, 6, 50–60.
3. Catalan, G., & Scott, J. F. (2009). Physics and applications of bismuth ferrite. *Adv. Mater*., *21*, 2463–2485. DOI: 10.1002/adma.200802849.
4. Gotardo, R. A. M., Viana, D. S. F., Olzon-Dionysio, M., Souza, S. D., Garcia, D., Eiras, J. A., Alves, M. F. S., Cotica, L. F., Santos, I. A., & Coelho, A. A. (2012). Ferroic states and phase coexistence in $BiFeO_3$-$BaTiO_3$ solid solutions. *J. Appl. Phys*., *112*(10), 104112–104112-7. DOI: 10.1063/1.4766450.
5. Park, T. -J., Papaefthymiou, G. C., Viescas, A. J., Lee, Y., Zhou, H., & Wong, S. S. (2010). Composition--dependent magnetic properties of $BiFeO_3$-$BaTiO_3$ solid solutions nanostructures. *Phys. Rev. B*, *82*, 024431-1-10. DOI: 10.1103/PhysRevB.82.024431.
6. Yang, S. -Ch., Kumar, A., Petkov, V., & Priya, S. (2013). Room-temperature magnetoelectric coupling in single-phase $BaTiO_3$-$BiFeO_3$ system. *J. Appl. Phys*., *113*, 144101-1-5. DOI: 10.1063/1.4799591.
7. Jartych, E., Malesa, B., Antolak-Dudka, A., & Oleszak, D. (2014). Mössbauer spectroscopy studies of multiferroic $(BiFeO_3)_{1-x}$-$(BaTiO_3)_x$ solid solutions prepared by mechanical activation. *Acta Phys. Pol. A*, *125*(3), 837–839. DOI: 10.12693/APhysPolA.125.837.
8. Malesa, B., & Mazurek, M. (2014). Hyperfine interactions in $(BiFeO_3)_{0.9}$-$(BaTiO_3)_{0.1}$ ceramics prepared by mechanical activation. *Informatyka, Automatyka, Pomiary w Gospodarce i Ochronie Środowiska*, 2, 16–19. (in Polish).
9. Goossenes, D. J., Weekes, C. J., Avdeev, M., & Hutchison, W. D. (2013). Crystal and magnetic structure of (1-x)$BiFeO_3$-x$SrTiO_3$ (x=0.2, 0.3, 0.4, and 0.8). *J. Solid State Chem*., *207*, 111–116. DOI: 10.1016/j.jssc2013.09.024.
10. Rachinger, W. A. (1948). A correction for the $\alpha_1\alpha_2$ doublet in the measurement of widths of X-ray diffraction lines. *J. Sci. Instrum*., *25*, 254–260. DOI: 10.1088/0950-7671/25/7/125.
11. Kowal, K., Jartych, E., Guzdek, P., Stoch, P., Wodecka-Duś, B., Lisińska-Czekaj, A., & Czekaj, D. (2013). X-ray diffraction, Mössbauer spectroscopy and magnetoelectric effect studies of $(BiFeO_3)_x$-$(BaTiO_3)_{1-x}$ solid solutions. *Nukleonika*, *58*(1), 57–61.
12. MacKenzie, K. J. D., Dougherty, T., & Barrell, J. (2008). The electronic properties of complex oxides of bismuth with the mullite structure. *J. Eur. Ceram. Soc*., *28*, 499–504. DOI: 10.1016/j.jeurceramsoc.2007.03.012.